

This discussion paper is/has been under review for the journal The Cryosphere (TC).  
Please refer to the corresponding final paper in TC if available.

# Surface energy budget on Larsen and Wilkins ice shelves in the Antarctic Peninsula: results based on reanalyses in 1989–2010

I. Välisuo<sup>1,2</sup>, T. Vihma<sup>1</sup>, and J. C. King<sup>3</sup>

<sup>1</sup>Finnish Meteorological Institute, Helsinki, Finland

<sup>2</sup>University of Helsinki, Department of Physics, Finland

<sup>3</sup>British Antarctic Survey, Cambridge, UK

Received: 29 January 2013 – Accepted: 1 March 2013 – Published: 27 March 2013

Correspondence to: I. Välisuo (ilona.valisuo@fmi.fi)

Published by Copernicus Publications on behalf of the European Geosciences Union.

Title Page

Abstract

Introduction

Conclusions

References

Tables

Figures

◀

▶

◀

▶

Back

Close

Full Screen / Esc

Printer-friendly Version

Interactive Discussion



## Abstract

Ice shelves in the Antarctic Peninsula have significantly disintegrated during the recent decades. To better understand the atmospheric contribution in the process, we have analysed the inter-annual variations in radiative and turbulent surface fluxes and weather conditions over Larsen C Ice Shelf (LCIS) and Wilkins Ice Shelf (WIS) in the Antarctic Peninsula in 1989–2010. Three atmospheric reanalyses were applied: ERA-Interim by ECMWF, Climate Forecast System Reanalysis (CFSR) by NCEP, and JRA-25/JCDAS by the Japan Meteorological Agency. In addition, in situ observations from an automatic weather station (AWS) on LCIS were applied, mainly for validation of the reanalyses. The AWS observations on LCIS did not show any significant temperature trend, and the reanalyses showed warming trends only over WIS: ERA-Interim in winter ( $0.23^{\circ}\text{Cyr}^{-1}$ ) and JRA in autumn ( $0.13^{\circ}\text{Cyr}^{-1}$ ). In LCIS from December through August and in WIS from March through August, the variations of surface net flux were partly explained by the combined effects of atmospheric pressure, wind, and cloud fraction. The explained variance was much higher in LCIS (up to 80%) than in WIS (26–27%). Summer melting on LCIS varied between 0 and 45 cm water equivalent (w.e.), which is comparable to previous results. The mean amount of melt days per summer on LCIS was only 17. The high values of melting in summer 2001–2002 presented in previous studies on the basis of simple calculations were not supported by our study. Instead, our calculations based on ERA-Interim yielded strongest melting in summer 1992–1993 on both ice shelves. On WIS the summer melting ranged between 2 and 40 cm w.e., and the peak values coincided with the largest disintegrations of the ice shelf.

## 1 Introduction

Ice shelves, floating extension of land ice, are found together with the glaciers and ice sheets with a marine terminal. They have complex interactions with atmosphere,

TCD

7, 1269–1311, 2013

Results based on  
reanalyses in  
1989–2010

I. Välisuo et al.

Title Page

Abstract

Introduction

Conclusions

References

Tables

Figures

◀

▶

◀

▶

Back

Close

Full Screen / Esc

Printer-friendly Version

Interactive Discussion



**Results based on  
reanalyses in  
1989–2010**

I. Välisuo et al.

Title Page

Abstract

Introduction

Conclusions

References

Tables

Figures



Back

Close

Full Screen / Esc

Printer-friendly Version

Interactive Discussion



ocean and the feeding glaciers. Ice shelves are sensitive to changes in atmospheric and oceanic circulation and temperatures. In the Antarctic Peninsula, the climate warming has been rapid during the last 50 yr and the total ice shelf area has reduced by over 28 000 km<sup>2</sup> (Cook and Vaughan, 2010). Despite of difficulties related to the large inter-annual variability and shortness of the time series (Chapman and Walsh, 1997), several studies have shown that the warming trend in the Antarctic Peninsula since 1950s has been stronger than the global average and the average over the rest of the Antarctic continent (King, 1994; Comiso, 2000; Vaughan et al., 2003; Turner et al., 2005; Chapman and Walsh, 2007). The long-term surface temperature trends have been largest on the west coast of Antarctic Peninsula (Sansom, 1989; Turner et al., 2005). The west coast has more manned observation stations, which increases the reliability of the trends observed. On the east coast of the Peninsula occupied observation stations are very few, but from the abrupt changes in the ice shelf area, it has been suggested that the east coast is also going through major climate changes (Turner et al., 2005).

The amplification of the warming in the area of Antarctic Peninsula has been linked, among others, to changing atmospheric or oceanic circulation, regional air-sea-ice feedbacks (Vaughan et al., 2003; King, 1994) and cloud cover variations (King, 1994). Changes in atmospheric circulation may increase warm-air advection from lower latitudes and enhance the föhn effect of the westerly winds. Changes in ocean circulation could increase the basal melting of the ice shelves. Air-sea-ice interactions and cloud radiative forcing have many ways to affect and respond to temperature variations. These connections are complicated and identifying the essential driving mechanism is difficult (King, 1994).

Ice shelves influence the global atmosphere-ocean-glacier-system in many ways. According to Glasser and Scambos (2008), calving through ice shelves accounts for 90 % of Antarctic ice mass loss, ice shelves influence the dynamics of inland ice and the ocean heat budget, and climatic perturbations cause collapses of ice shelves. The ice shelves are also connected to sea level rise: studies have found evidence of accelerated glacier flow and glacier surges after ice sheet collapse (Rott et al., 2002;

**Results based on  
reanalyses in  
1989–2010**

I. Välisuo et al.

Title Page

Abstract

Introduction

Conclusions

References

Tables

Figures

◀

▶

◀

▶

Back

Close

Full Screen / Esc

Printer-friendly Version

Interactive Discussion



De Angelis and Skvarca, 2003), which could contribute to the eustatic sea level rise. The break up mechanisms of ice shelves are not fully understood and many factors have been suggested to take part in the collapse. For example glaciological discontinuities (Braun et al., 2009), surface melting and melt ponds (Braun et al., 2009, van den Broeke, 2005), and capsize mechanism (Braun et al., 2009) are believed to be important in the break-up process. The collapses of the ice shelves are believed to be partly caused by atmospheric warming (Rott et al., 1998; Scambos et al., 2000; Shepherd et al., 2003) and increased surface melting (van den Broeke, 2005). Van den Broeke (2005) mentions more specifically the increase of warm-air advection and strengthening of the föhn effect, caused by a perturbation in atmospheric circulation, to have their share in the decrease of ice shelf area in the Antarctic Peninsula. The effect of ocean temperature has also been pointed out in several studies (Rott et al., 1998; Scambos et al., 2000; Shepherd et al., 2003; Braun et al., 2009). The sea ice concentration might also be related to the state of the ice shelves, but the connection or feedback is believed to be rather complicated (van den Broeke, 2005).

A recent study by Kuipers Munneke et al. (2012) addressed the weather conditions on Larsen C Ice Shelf (LCIS, Fig. 1) and their effect on the ice shelf surface net flux. They analysed the weather variables measured by two automatic weather stations. The observations were also used as input for a surface energy balance model. The model calculations and observations together suggested that the subsurface absorption of solar radiation was important. The penetration of solar radiation increased subsurface melting and decreased surface melting, the former being dominant, thus leading to a larger net melt. Kuipers Munneke et al. (2012) also drew attention on the connection between westerly winds and weather conditions on LCIS. Moderate or strong westerly flow over the Peninsula leads to northerly flow to the west of the Peninsula (Orr et al., 2004), together with föhn winds, cloudless skies and advection of warm and dry air on the eastern side of the Peninsula (Marshall et al., 2006; van Lipzig et al., 2008). According to Kuipers Munneke et al. (2012), when the cloud cover was reduced, the

increase of shortwave radiation and sensible heat flux outweighed the decrease of longwave radiation and latent heat flux.

In the previous studies addressing to the evolution of ice shelves, different limits for the viability of the ice shelves have been proposed. Many have agreed that the annual mean near-surface temperature should be  $-9^{\circ}\text{C}$  or lower for an ice shelf to survive (Mercer, 1978; Vaughan and Doake, 1996; Vaughan et al., 2003; Rott et al., 1996, 1998; Morris and Vaughan, 2003). Also the summertime isotherm of  $0^{\circ}\text{C}$  has been suggested to be the temperature limit below which the ice shelves would be viable (Mercer, 1978). In year 2000, the  $-9^{\circ}\text{C}$  annual isotherm crossed the south-western parts of Wilkins Ice Shelf (WIS) on the western side of the Peninsula and on Jason Peninsula on the eastern side. Larsen B Ice Shelf on the northern side of Jason Peninsula had an annual mean temperature higher than  $-9^{\circ}\text{C}$  and LCIS and Larsen D on the southern side were colder than  $-9^{\circ}\text{C}$  (Cook and Vaughan, 2010).

LCIS and WIS are located about 300–400 km apart, and experience remarkably different weather conditions. The west side of the Peninsula, where WIS is located, is exposed to the warm and humid westerly winds from the Southern Ocean. On the eastern side of the Peninsula, Larsen Ice Shelves are confronting colder and drier climate due to the continental air masses flowing from West Antarctica and Coats Land to Ronne Ice Shelf and further to the Weddell Sea (King and Turner, 1997). Furthermore, LCIS and WIS have different structure and mechanical characteristics (Braun et al., 2009).

In January 2008 the area of the WIS was  $13\,000\text{ km}^2$ , which was reduced by almost  $2000\text{ km}^2$  by the collapses in February, May and June. In April 2009 an ice bridge connecting the ice shelf to Charcot Island gave in. WIS gains mass mainly by direct accumulation and loses mass by basal melt (Braun et al., 2009). Some zones on the ice shelf also encounter intense surface melting. The mean horizontal velocities on the ice shelf are very small, but the accumulation rate in WIS is relatively high. WIS is characterised by a very large number of ice rises and by connections to the confining islands. The bulk temperature of the ice is high on WIS, which indicates a weaker ice

Results based on  
reanalyses in  
1989–2010

I. Välisuo et al.

Title Page

Abstract

Introduction

Conclusions

References

Tables

Figures

◀

▶

◀

▶

Back

Close

Full Screen / Esc

Printer-friendly Version

Interactive Discussion



matrix (Braun et al., 2009). During the last decades WIS has experienced several major break-up events ranging from 20 to 1200 km<sup>2</sup> (Braun et al., 2009).

The surface area of LCIS is 51 000 km<sup>2</sup>, which makes it the largest ice shelf on Antarctic Peninsula (Cook and Vaughan, 2010). It has twelve major flow units or ice shelf domains (Glasser et al., 2009). Contrary to WIS, the input glaciers are fast flowing and contribute actively to the mass balance of the ice shelf (Glasser et al., 2009). On the ice shelf, two main kinds of rift systems are observed: tributary glacier rift systems and ice shelf edge rifts. No large-scale changes in the location of rifts and crevasses have been observed between 2002 and 2007, at least. The overall changes in the ice shelf have been small during the last two decades, although the ice shelf edge shows a gradual recession. On the basis of the residence time of the ice on the ice shelf, it has been estimated that LCIS has existed in its present configuration for at least 560 yr (Glasser et al., 2009). In future LCIS is supposed to stay stable with cyclical calving and regrowth; an imminent collapse of LCIS is found unlikely (Glasser et al., 2009). Future changes could be dominated by gradual thinning of the ice shelf (Shepherd et al., 2003).

In this paper, the weather conditions and surface fluxes on LCIS and WIS are studied using atmospheric reanalyses. Our primary objective is to find out (1) how the net surface heat flux (sum of radiative and turbulent surface fluxes) varies inter-annually, (2) how the flux variations are related to large-scale weather conditions, and (3) how much summer melt the net heat flux generates, and (4) how the summer melt varies inter-annually and compares with the observed disintegration events of the ice shelves.

## 2 Material and methods

### 2.1 Atmospheric reanalyses

In atmospheric reanalyses the majority of available observations is combined with state-of-the-art modelling solutions to obtain the best estimate for the real state of

TCD

7, 1269–1311, 2013

Results based on  
reanalyses in  
1989–2010

I. Välisuo et al.

Title Page

Abstract

Introduction

Conclusions

References

Tables

Figures

◀

▶

◀

▶

Back

Close

Full Screen / Esc

Printer-friendly Version

Interactive Discussion



climate in the past and present. The advantages of reanalyses are good temporal and spatial coverage, as well as good consistency. In reanalyses, errors and artificial trends caused by model and data assimilation changes are avoided, but changes in observation systems can cause complications (Saha et al., 2010; Bengtsson et al., 2007). Saha et al. (2010) emphasize that one single reanalysis does not suffice due to changes in observations and input data, and due to the different possibilities in models and data assimilation solutions.

In this study we apply three reanalyses: ERA-Interim (Dee et al., 2011), NCEP-CFSR (Saha et al., 2010) and JRA-25 (Onogi et al., 2007). ERA-Interim (ERA-Interim), a reanalysis by the European Centre for Medium Range Weather Forecasts (ECMWF), has been created as an intervening step between the former ERA-40 reanalysis and an upcoming reanalysis. When this study was started, ERA-Interim covered the years from 1989 to 2010. Its horizontal resolution is 79 km and it has 60 vertical levels. ERA-Interim applies four-dimensional variational data assimilation (4D-VAR). Climate Forecast System Reanalysis, CFSR, is developed by the National Centres for Environmental Prediction (NCEP), USA. Its time range is from 1979 to present. The horizontal resolution is 38 km and the number of vertical levels is 64. The data assimilation technique is 3D-VAR. The Japanese Reanalysis 25 was conducted in collaboration with Japan Meteorological Agency (JMA) and the Central Research Institute of Electric Power Industry (CRIEPI). The reanalysis was first made for a 25-yr period from 1979 to 2004 after which it was continued with an identical set-up from 2005 to present. The continuation part is called JCDAS. From here we will call both parts of the reanalysis as JRA. The horizontal resolution of JRA is 120 km and the number of vertical model levels is 40. A recent study by Cullather and Bosilowich (2012) noted that ERA-Interim and CFSR have better surface parametrisation than the novel NASA-MERRA reanalysis. Despite the good parametrisations, ERA-Interim and CFSR disagree with observations of surface fluxes and atmospheric boundary-layer variables in polar regions (Cullather and Bosilowich, 2012; Jakobson et al., 2012).

**Results based on reanalyses in 1989–2010**

I. Välisuo et al.

Title Page

Abstract

Introduction

Conclusions

References

Tables

Figures

◀

▶

◀

▶

Back

Close

Full Screen / Esc

Printer-friendly Version

Interactive Discussion



**Results based on  
reanalyses in  
1989–2010**

I. Välisuo et al.

Title Page

Abstract

Introduction

Conclusions

References

Tables

Figures

◀

▶

◀

▶

Back

Close

Full Screen / Esc

Printer-friendly Version

Interactive Discussion



Radiative and turbulent surface fluxes and basic weather variables were collected from the three reanalyses. We used the monthly mean products, and further calculated annual and seasonal means for summer (December–February), autumn (March–May), winter (June–August), and spring (September–November). The areal means over LCIS and WIS were calculated for each variable. This was done by selecting the relevant grid points for LCIS and WIS and calculating the mean value from those. Since all the three reanalyses had different resolution, the areal averaging was done individually for each reanalysis. To have a consistent base for the study, only such grid points were included which lie on the presently existing parts of the ice shelves. As the low resolution of the reanalyses smoothes the orography of the Antarctic Peninsula, part of the chosen grid points lie at higher elevations in the reanalyses than the actual level of the ice shelf in nature.

## 2.2 Observations

The validation of reanalyses was done using data from an automatic weather station (AWS) on LCIS. The AWS is located at 67.012° S, 61.55° W and operated by the British Antarctic Survey. The AWS measurements are compared against the nearest grid point in the reanalyses. The station was initially deployed in October 1985 and has been in operation ever since. The AWS measures air temperature, pressure, wind speed and direction, and relative humidity, but neither radiative nor turbulent surface fluxes.

## 2.3 Validation of reanalyses

Our primary objective in validation is to understand how well the three reanalyses can reproduce the observed inter-annual variations over the ice shelves. Results of ERAI, CFSR and JRA were compared against the AWS observations on the air temperature and horizontal wind components. The wind was observed at the height at 3 m above the snow surface, whereas the reanalyses output was from the height of 10 m. A height correction was done applying the logarithmic wind profile, assuming an aerodynamic

roughness length of 1 cm (no information on stability was available). No height correction was calculated to air temperature, because the height difference between the measured values (height of 3 m) and reanalysis outputs (2 m) was so small. The validation was performed for the seasonal averages from autumn 1989 to spring 2010.

The results for the seasonal means reveal that for the near-surface temperature, the best performance, ranked on the basis of bias and root-mean-squared error (RMSE), is achieved in summer (December–February, Table 1). The summertime temperature correlations range from 0.43 (ERA-I) to 0.61 (CFSR). The correlation for ERA-I is even better (0.71) in winter, June–August, but the biases of all reanalyses are more than doubled compared to summer (Table 1). The eastward wind component ( $U$ ) performs best in summer, although the wintertime performance is almost as good. The northward component ( $V$ ) has clearly the best performance in summer. For  $U$ , the biases are positive, i.e. all reanalyses overestimate the strength of the westerly wind on LCIS. For  $V$  the bias is mostly negative. JRA stands out for the highest correlations for the  $U$  component, although the temperature and  $V$  wind correlations are mostly weaker than for ERA-I and CFSR.

As a summary, the capability of reanalyses to reproduce the observed inter-annual variations (of seasonal means) was found satisfactory for the air temperature, but worse for the wind. We note that also AWS observations are liable to errors, which may be caused, among others, by solar heating of the temperature sensors as well as snow and ice accretion in the anemometer. Hence, the results presented in Table 1 contain uncertainties, but should give an idea on the relative performance of the three reanalyses, in particular when we focus on the correlations. This is because observation errors most probably do not increase correlations, although in some cases they may reduce the bias and RMSE.

**Results based on reanalyses in 1989–2010**

I. Välisuo et al.

Title Page

Abstract

Introduction

Conclusions

References

Tables

Figures

◀

▶

◀

▶

Back

Close

Full Screen / Esc

Printer-friendly Version

Interactive Discussion



### 3 Results on temporal evolution

Our focus is on the surface energy fluxes and weather conditions on LCIS and WIS. The investigation of surface fluxes is limited to net solar radiation, net thermal radiation, sensible heat flux and latent heat flux, which together describe the heat exchange between the surface and the atmosphere. The sub-surface heat flux, i.e. the conductive heat flux between the surface and deeper layers in the snow, was not taken into account. The weather variables in consideration are the 2-m air temperature, 10-m wind components, and mean sea level pressure. The time series of monthly mean values are presented and trends of seasonal and annual mean values are calculated. Notice is taken of the weather conditions favouring particularly large or small surface energy fluxes.

#### 3.1 Time series

The time series of surface energy fluxes are presented in Fig. 2. The turbulent fluxes of sensible and latent heat are small in each reanalyses and on both ice shelves. They are of opposite sign throughout the year, the sensible heat flux being towards the snow surface (defined as the positive direction) and the latent heat flux from snow to air (negative). The net solar radiation differs a lot between the three reanalyses. The lowest summertime net solar radiations are obtained from CF SR and the largest ones from JRA. The values from ERA are close to those of CF SR, but show a much larger inter-annual variation. The net solar radiation has a tendency of being slightly larger on WIS than on LCIS. The net thermal radiation is of the same magnitude in all reanalyses and both areas. The mean net thermal radiation is slightly stronger in JRA than in the two other reanalyses.

The net flux varies on both sides of zero in all reanalyses. There are major differences in the seasonal cycle of the net flux between the reanalyses and regions. ERAI shows the largest interannual variation in the net flux, but the mean values are comparable to the other reanalyses. In CF SR and JRA the net flux is almost identical every year.

Title Page

Abstract

Introduction

Conclusions

References

Tables

Figures



Back

Close

Full Screen / Esc

Printer-friendly Version

Interactive Discussion



Interestingly, CFSR produces a very small net flux on LCIS, but a relatively large one on WIS. JRA also produces a larger interannual variation on WIS than on LCIS, but the difference between the two areas is smaller than in CFSR. The 20-yr seasonal mean values of the surface fluxes reveal that the fluxes vary more between the reanalyses than between the areas (Table 2).

All the three reanalyses show a roughly similar behaviour in 2 m temperature (Fig. 3). The largest differences between the reanalyses are obtained in summer and winter, whereas in spring and autumn the reanalyses are in good agreement. In summer, only ERAI reaches or rises clearly above the melting point on LCIS. On WIS the maximum monthly mean temperature was 1 °C on both ERAI and JRA reanalyses. While JRA produces almost as warm summers as ERAI, but CFSR is every summer 2 to 5 °C colder than ERAI. In winter CFSR gives the highest temperatures, i.e. it yields the smallest annual temperature cycle, both on LCIS and WIS. All the three reanalyses give relatively similar variability of the wind components (Fig. 3). JRA shows highest variability in wind, especially in the U-component. JRA also has a stronger V-component of the wind on LCIS and weaker on WIS than ERAI and CFSR. The mean sea level pressure is almost identical in all reanalyses compared, and the pressure variations are almost similar on LCIS and WIS.

### 3.2 Trends

The air temperature and wind observations at the AWS on LCIS showed trends neither in annual nor seasonal means. JRA results agreed on this, and the trends in wind components in ERAI and CFSR were small, although statistically significant (Table 3). On WIS, however, ERAI and JRA showed clear warming trends but in different seasons: ERAI in winter (0.23 K yr<sup>-1</sup>) and JRA in autumn (0.13 K yr<sup>-1</sup>, Table 3).

Considering surface fluxes, the annual means included statistically significant trends mostly on WIS, but most of these were so small that they are practically immeasurable (Table 3). For the net heat flux, only CFSR included a minor increasing trend on LCIS.

Title Page

Abstract

Introduction

Conclusions

References

Tables

Figures



Back

Close

Full Screen / Esc

Printer-friendly Version

Interactive Discussion



## Results based on reanalyses in 1989–2010

I. Välisuo et al.

Title Page

Abstract

Introduction

Conclusions

References

Tables

Figures

◀

▶

◀

▶

Back

Close

Full Screen / Esc

Printer-friendly Version

Interactive Discussion



Several seasonal trends were found (Table 3). In LCIS, ERAI showed seasonal trends in autumn in latent heat flux and net heat flux. ERAI also showed a negative trend in net thermal radiation in DJF. JRA had trends in latent heat flux and net heat flux in LCIS, but in different season than ERAI. The trends in latent heat flux were weak and seen in spring and summer. The trend in the net heat flux was observed in summer. In CFSR, on LCIS, the net heat flux had a trend in autumn, winter and spring. All of them showing rising net heat flux.

More seasonal trends were found over WIS. As for LCIS, the three reanalyses did not agree in the season and magnitude of the trends. One should note especially that ERAI presented a strong negative trend on the net heat flux in autumn ( $-0.55 \text{ Wyr}^{-1}$ ), winter ( $-0.78 \text{ Wyr}^{-1}$ ) and spring ( $-0.74 \text{ Wyr}^{-1}$ ), which were not present in JRA and CFSR. Instead, JRA had a positive trend in the net heat flux ( $0.21 \text{ Wyr}^{-1}$ ) in autumn.

### 3.3 Weather condition favouring large and small surface net fluxes

As shown in Sect. 3.1, the inter-annual variation in surface net flux is largest in ERAI, whereas CFSR and JRA show very little inter-annual variations in the surface net flux. Hence, the analyses in this Section are based on ERAI only. Differences between the years are clearly larger on LCIS than on WIS. On LCIS some summers show an exceptionally high net flux and some winters have an exceptionally low surface net flux. Summers with strikingly low, or winters with especially high surface net flux were not observed. Next we investigate a summer with high net energy flux and a winter with low energy flux on LCIS. The mean synoptic conditions during these periods are presented and compared to the usual conditions.

#### 3.3.1 Weather conditions favouring a large summertime net heat flux

Summer 1992–1993 was characterised by an exceptionally high surface net flux on LCIS. In Figs. 4–7, the maps of December–February mean values of sea level pressure, wind speed, cloudiness and surface temperature are presented for summer

1992–1993. For comparison, similar maps are shown also for summer 1999–2000. This reference summer was selected by comparing all summer situations to the two decade mean summer synoptic situation; summer 1999–2000 was most similar to the mean situation.

5 On LCIS the atmospheric pressure was 10 hPa higher in summer 1992–1993 than in summer 1999–2000 (Fig. 4). In summer 1992–1993 the low pressure minimum was situated on the west side of the Peninsula, in the Bellingshausen Sea (the whole low pressure structure is not visible in Fig. 4 due to the limited area of the map). The pressure increases steadily towards north-east. In summer 1999–2000, a low was situated  
10 on the west side of the Peninsula, but also another, slightly weaker, low was seen on the east side of the Peninsula in the Weddell Sea. The lows were connected by a saddle in the middle part of the Peninsula at around 66 to 68° S. During this summer, the pressure increased rather evenly towards north and south, whereas in summer 1992–1993 the pressure gradient was in a north-east–south-west direction.

15 In summer 1992–1993 the winds were predominantly northwesterly (Fig. 5). The wind speed on LCIS was from 2 to 8 ms<sup>-1</sup>, being in the eastern parts of the ice shelf slightly stronger than during the reference summer 1999–2000. The reference summer was characterized by the lack of northerly wind component in the eastern side of the Peninsula. In summer 1999–2000 the mean wind speed on LCIS was almost  
20 uniformly from the west. The cloud coverage on LCIS was eight percentage points higher in 1992–1993 than in 1999–2000 (Table 4, Fig. 6). The increase of cloud fraction coincided with a decrease of downward shortwave radiation and increase of downward longwave radiation (Table 4). As the cloud forcing on net radiation was positive throughout the year (with a minimum of 15 Wm<sup>-2</sup> in January), also the net radiation  
25 increased. Largest differences in the surface skin temperature occurred on the north-eastern coast and south-eastern corner of the Peninsula (Fig. 7). On the north-eastern coast the -2°C isotherm moved poleward in summer 1992–1993, so that the major part of LCIS surface was warmer than -2°C. In summer 1999–2000, the mean skin temperature of LCIS was between -2°C and -4°C.

---

**Results based on  
reanalyses in  
1989–2010**I. Välisuo et al.

---

Title Page

Abstract

Introduction

Conclusions

References

Tables

Figures

◀

▶

◀

▶

Back

Close

Full Screen / Esc

Printer-friendly Version

Interactive Discussion



### 3.3.2 Weather conditions favouring a small wintertime net heat flux

During winter 1991 the surface net flux on LCIS was lower than usual. The winter (June, July, and August) mean weather conditions in the vicinity on Antarctic Peninsula are presented in Figs. 8–11. Winter 1996 was chosen as a reference, by similar grounds as summer 1999–2000 in the summer season comparison.

In winter 1991 a low pressure centre was situated in the Weddell Sea, whereas in winter 1996 it was situated in the Bellingshausen Sea (Fig. 8). In 1991 the atmospheric pressure on LCIS was about 4 hPa lower than in winter 1996. The pressure gradients over the ice shelf were weak during both winter. In winter 1991, the wind had a predominantly westerly direction having a small southerly component on LCIS and southerly winds with cold-air advection were dominant further north than in the reference winter (Fig. 9). During the reference winter, the mean wind was from the west with a small northerly component on the western side of the Peninsula and southerly component on the eastern side. The wind field on LCIS did not differ much during the two winters.

The cold winter 1991 with a higher atmospheric pressure is was related to drier and less cloudy conditions than winter 1996 (Fig. 10). On LCIS, the mean cloud fraction was 68 % in winter 1991 and 75 % in winter 1996. With the lower cloud coverage the incoming longwave radiation was weaker and the net surface radiation lower by  $-28 \text{ W m}^{-2}$ . In winter 1991 the mean surface skin temperature was lower than in 1996; on LCIS and the Weddell Sea the difference was as much as about  $5^\circ\text{C}$  (Fig. 11).

### 3.3.3 Multiple regression analysis on surface net flux and weather conditions

Multiple regression analysis was applied to quantitatively investigate how the atmospheric pressure, horizontal wind components, wind speed, and cloud fraction affected the surface net heat flux during the whole study period of 1989–2010. In some seasons, the analysis yielded statistical relationships with a high degree of explanation (Table 5). The results were better for LCIS than WIS. On LCIS the wind speed, either of the wind components, and air temperature together explained 58 to 80 % of the

Title Page

Abstract

Introduction

Conclusions

References

Tables

Figures



Back

Close

Full Screen / Esc

Printer-friendly Version

Interactive Discussion



variance of the surface net flux in summer, autumn, and winter (in cases when one wind component and wind speed are both included in the equation, we checked that the explaining variables were independent, i.e. had a low mutual correlation). In spring, on neither LCIS nor WIS the variation in the net flux was explained by the weather variables. By showing statistically significant correlations during 1989–2010 between the net heat flux and weather variables, the multiple regression analysis confirms the conclusions made on the basis of the extreme summer and winter. Among the essential weather variables (Table 5), only the effect of the wind speed was not evident in the analyses of the extreme summer and winter.

### 3.4 Summertime surface melting

Summertime melting of snow on LCIS and WIS were calculated using the surface temperature and surface fluxes of ERAI. We only applied ERAI because (a) the inter-annual variations in the net flux in the other two reanalyses were very small and (b) in CFSR the monthly mean surface temperature did not reach the melting point, but ranged mostly between  $-2$  and  $-4^{\circ}\text{C}$  in every summer. Our method to determine the melting resembled that of van den Broeke (2005). The melt calculations were done in 12-h steps. Using the 12-h stepping may underestimate melting, but as the calculations are done identically for each year, the results provide relevant information on the inter-annual variations. ERA-Interim also provides 3-h forecasts for the surface fluxes, but these appeared unrealistic with negative net fluxes in summer (possibly due to errors in the forecast initialization), and thus 12-h forecasts were chosen for melt calculations. The criteria for melting was the following: if the surface temperature at the end of the 12-h step reached  $0^{\circ}\text{C}$ , the 12-h period was considered as a melting period. We assumed that during these periods the surface net flux was used directly for melting the snow as the surface temperature was already at the melting point. The energy available for melting,  $M$ , was calculated using

$$M = SW + LW + SH + LH \quad (1)$$

Title Page

Abstract

Introduction

Conclusions

References

Tables

Figures

◀

▶

◀

▶

Back

Close

Full Screen / Esc

Printer-friendly Version

Interactive Discussion





based on atmospheric reanalyses, which have weaknesses in high latitudes. Our study revealed significant differences between ERAI, CFSR and JRA on LCIS and WIS.

According to our knowledge, near-surface variables of reanalyses have not been previously validated over Antarctic Peninsula ice shelves, as previous validation studies of atmospheric reanalyses in the Antarctic have mostly focused on large-scale features, such as cyclones (Hodges et al., 2011) and precipitation (Bromwich et al., 2011). The validation against the AWS observations on LCIS demonstrated that ERAI can reasonably well reproduce the observed inter-annual variations of seasonal mean air temperature for winter, spring and summer, whereas CFSR is good for summer and spring, and JRA for summer. For the wind components, the correlations were lower on average. We note, however, that also AWS observations are liable to errors, which may have lowered the correlation coefficients. Focusing on biases of seasonal means, our validation results include interesting aspects: (1) all three reanalyses had warm temperature biases in all seasons, (2) all three reanalyses yielded positive biases for the eastward wind component in all seasons, and (3) reanalyses mostly yielded negative biases for the northward wind component. Issue (1) is in agreement with many previous validation studies over snow and ice surfaces: Jakobson et al. (2012) got similar results for the same (and other) reanalyses over the Arctic sea ice, and Vihma et al. (2002) observed a year-round warm bias for the ECMWF operational analyses over the Antarctic sea ice, and Atlaskin and Vihma (2012) observed that several numerical weather prediction models yielded warm biases under conditions of stable boundary layer over snow-covered boreal forest. Issues (2) and (3) are probably at least partly due to the resolution of reanalyses, which is not high enough to accurately represent the complex orography of the Antarctic Peninsula. This results in overestimation of westerly winds blowing over the Peninsula (Stössel et al., 2011), and these strong westerlies and reduced generation of barrier winds results in an underestimation of the northward wind component. This also means that the reanalyses will not properly represent the formation of föhn winds on the eastern side of the Peninsula, which are believed to be important in promoting melt on LCIS (Marshall et al., 2006). The reanalysis products

Results based on  
reanalyses in  
1989–2010

I. Välisuo et al.

Title Page

Abstract

Introduction

Conclusions

References

Tables

Figures

◀

▶

◀

▶

Back

Close

Full Screen / Esc

Printer-friendly Version

Interactive Discussion



## Results based on reanalyses in 1989–2010

I. Välisuo et al.

Title Page

Abstract

Introduction

Conclusions

References

Tables

Figures

◀

▶

◀

▶

Back

Close

Full Screen / Esc

Printer-friendly Version

Interactive Discussion



can also be compared against the AWS observations of Kuipers Munneke et al. (2012) from LCIS in February 2009–January 2011. In all three reanalyses in all seasons, the net shortwave radiation was larger than in the AWS data. Also the net longwave radiation, which was negative year-round, had a larger magnitude in the reanalyses. Also the turbulent sensible heat flux was larger (and positive around the year) in the reanalyses than in the AWS data, and the latent heat flux, which was negative year-round in the reanalyses, had a larger magnitude in the reanalyses than in the AWS data. At the latter, the latent and sensible heat fluxes changed sign in the course of the year. The net flux (sum of radiative and turbulent fluxes) presented by Kuiper Munneke et al. (2012) was much closer to zero than in any of the three reanalyses. We note, however, that the AWS observations of radiative fluxes may include errors due to accumulation of frost, condensed water, and snow in the domes of the radiation sensors. Further, the turbulent fluxes were not directly measured but parameterized on the basis of observations on the air and surface temperature, air humidity, and wind speed, which reduces their accuracy.

Also the comparison of the three reanalyses over LCIS and WIS yielded interesting results. The time series of the mean sea level pressure were almost identical in the three reanalyses both on LCIS and WIS. The monthly mean sea level pressure also had consistent variation on both sides of the Peninsula. On the contrary, the summer-time 2-m air temperature on LCIS differed remarkably between ERAI and CFSR. ERAI reached the melting point every summer, whereas the summer temperatures of CFSR were typically from  $-4$  to  $-2^{\circ}\text{C}$ , which hardly allows summer melt (for sub-surface melt, see below). The ERAI mean wind speeds were about  $3\text{ ms}^{-1}$  higher than those of CFSR. JRA had very different wind speed variations than ERAI and CFSR, both on LCIS and WIS. The most striking differences in surface fluxes were related to the very large solar radiation in JRA on WIS.

In general, ERAI had larger inter-annual variations compared to the almost uniform years in CFSR. This suggests that the patterns in ERAI are more realistic, considering the observations on large inter-annual variability in the Peninsula region (King, 1994;

## Results based on reanalyses in 1989–2010

I. Välisuo et al.

Title Page

Abstract

Introduction

Conclusions

References

Tables

Figures

◀

▶

◀

▶

Back

Close

Full Screen / Esc

Printer-friendly Version

Interactive Discussion



Vaughan et al., 2003). Although ERAI has much more coarse horizontal resolution (79 km) than CFSR (38 km), it has the clear advantage of applying the 4D-VAR data assimilation, which is not used in CFSR and JRA. Although JRA performed poorly in the temperature validation, it was the best reanalysis for the zonal wind component. In the Arctic, Jakobson et al. (2012) have noticed the good quality of JRA winds. In general, ERAI was found to be the most appropriate reanalysis for more specific studies of the weather patterns.

When the summertime surface net heat flux on LCIS was exceptionally high (1992–1993), the mean sea level pressure in the vicinity of the Peninsula was higher than general, and the pressure difference between the east and the west side of the Peninsula was greater. Due to the anomalous pressure field, the surface winds were from north-west on the eastern side of the Peninsula. The warm-air advection together with strong solar insolation under reduced cloud cover contributed to the high air and snow surface temperatures on LCIS. Also previous studies have indicated that high temperatures on Larsen ice shelf were found together with northwesterly winds (Kuipers Munneke et al., 2012) and the break up of Larsen B ice shelf in 2002 was preceded by northwesterly winds (van den Broeke, 2005). During the winter with anomalously small surface net energy flux, the mean sea level pressure was higher than on average winters. This tends to reduce the cloud cover, which results in weaker cloud radiative forcing, allowing the surface to cool more. During winter 1991 of low surface net flux, the pressure field was also significantly different from regular winters and summers. The lowest pressures were situated in the Weddell Sea, forcing the southerly winds in the vicinity of the Peninsula. The surface temperatures were lower, likely due to cold-air advection and strong radiative cooling.

The climate warming in the Peninsula region (e.g. King, 1994; Vaughan et al., 2003) was not as clearly present in our results as could have been expected. The AWS observations on LCIS did not include any significant temperature trend, and the reanalyses showed warming trends only over WIS: ERAI in winter ( $0.23\text{ }^{\circ}\text{C yr}^{-1}$ ) and JRA in autumn ( $0.13\text{ }^{\circ}\text{C yr}^{-1}$ ). Also, according to previous assumptions on the climate evolution

in the Peninsula region (e.g. Kuipers-Munneke, 2012), trends on wind would have been awaited. The AWS data did include trends in scalar wind speed in all seasons except summer (DJF), but all these trend were negative indicating a decrease in wind speed on LCIS. The statistically significant trends (95% level) in autumn, winter and spring were about  $-0.2$  ( $\text{ms}^{-1} \text{yr}^{-1}$ ). The annual mean wind speed did not have a trend of any sign. Among reanalyses only CFSR showed trends: in the eastward component in summer on LCIS ( $+0.03$  ( $\text{ms}^{-1} \text{yr}^{-1}$ )) and WIS ( $+0.03$  ( $\text{ms}^{-1} \text{yr}^{-1}$ )).

Our calculations for LCIS yielded 5 to 72 melt days per summer, whereas van den Broeke (2005) estimated much more, from 50 to 100 melt days per summer for the same area. Comparing the same period as van den Broeke (2005), from 1995 to 2003, our result for the average number of melt days was 17 per summer, whereas van den Broeke got 69. For the same period, we calculated the summer melt to range from 0 to 45 cm, whereas van den Broeke got 10 to 42 cm. Hence, the differences were much larger in the number of melt days than in the total melt during a summer. These must be related to the five differences in the calculation methods (Sect. 3.4). One of them was that we defined the melting according to the ERAI surface temperatures, whereas van den Broeke used the air temperature measured at the boom height (3m) of the AWS. The surface-based temperature inversion, common on polar regions also during summer, may partly explain the higher number of melt days in van den Broeke (2005), as the air temperature is higher than the snow surface temperature. Also, ignoring the latent heat flux may have yielded too much melting in van den Broeke (2005). We note that neither we nor van den Broeke (2005) took into account the absorption of solar radiation into the snow. The penetration of shortwave radiation into the snow changes the partitioning between surface and subsurface melt, and increases the total melt (Cheng et al., 2008; Kuipers Munneke et al., 2012).

Van den Broeke stated that melting in summer 2001–2002 was exceptionally strong on LCIS. We did not observe the same, but instead noted increased melting in 2002–2003. Outside of van den Broeke’s study period, summer 1992–1993 stands out with strong melting on both LCIS and WIS. The final disintegrations of Larsen A and Prince

**Results based on reanalyses in 1989–2010**

I. Välisuo et al.

Title Page

Abstract

Introduction

Conclusions

References

Tables

Figures

◀

▶

◀

▶

Back

Close

Full Screen / Esc

Printer-friendly Version

Interactive Discussion



Gustav ice shelves happened in early 1995 (Rott et al., 1996; Cooper, 1997; Cook and Vaughan, 2010) following the record high melt in 1992–1993. On WIS the peak values in melting in summers, based on our calculations, seem to agree with the major collapses in 1990–1991, 1993, 1998, 2003–2004 (Braun et al., 2009). Nevertheless, a major collapse occurred also in 2008, when the melting was modest, and in 2006 the area of WIS did not change much despite of the strong melting.

We conclude that atmospheric reanalyses provide useful information on the surface energy budget and melt of Antarctic ice shelves, on inter-annual variations in the budget terms, and on the weather conditions associated with high and low net heat flux to the ice shelves. Care should, however, been taken when making conclusions on the basis of reanalysis products; in our case the validation and comparison of three reanalyses were essential. As a whole, our results support the idea that the recent disintegrations of Larsen Ice Shelves and WIS are partly of atmospheric origin. As the next step, we consider important to carry out more detailed melt calculations applying a thermodynamic snow model, forced by atmospheric reanalyses, accounting for the role of subsurface melting.

*Acknowledgements.* This study was supported by the Academy of Finland through the AM-ICO project (contracts 128533 and 263918). The ECMWF, JMA, and NCEP are acknowledged for providing us with the reanalysis products. The automatic weather station measurements were funded by the UK Natural Environment Research Council as part of the British Antarctic Survey's core programme "Polar Science for Planet Earth". This publication is contribution number 19 of the Nordic Centre of Excellence SVALI, "Stability and Variations of Arctic Land Ice", funded by the Nordic Top-level Research Initiative (TRI).

**Results based on reanalyses in 1989–2010**

I. Välisuo et al.

Title Page

Abstract

Introduction

Conclusions

References

Tables

Figures



Back

Close

Full Screen / Esc

Printer-friendly Version

Interactive Discussion



## References

- Andreas, E. L., Jordan, R. E., and Makshtas A. P.: Simulations of snow, ice and near-surface atmospheric processes on Ice Station Weddell, *Journal of Hydrometeorology*, 5, 611–624, 2004.
- 5 Andreas, E. L., Jordan, R. E., and Makshtas A. P.: Parameterizing turbulent exchange over sea ice: the Ice Station Weddell results, *Bound.-Lay. Meteorol.*, 114, 439–460, 2005.
- Atlaskin E. and Vihma T.: Evaluation of NWP results for wintertime nocturnal boundary-layer temperatures over Europe and Finland, *Q. J. Roy. Meteorol. Soc.*, 138, 1440–1451, 2012.
- 10 Bengtsson, L., Arkin, P., Berrisford, P., Bougeault, P., Folland, C. K., Gordon, C., Haines, K., Hodges, K. I., Jones, P., Kållberg, P., Raynes, N., Simmons, A. J., Stammer, D., Thorne, P. W., Uppala, S., and Vose R. S.: The need for a dynamical climate reanalysis, *B. Am. Meteor. Soc.*, 88, 495–501, 2007.
- Braun, M., Humbert, A., and Moll, A.: Changes of Wilkins Ice Shelf over the past 15 years and inferences on its stability, *The Cryosphere*, 3, 41–56, doi:10.5194/tc-3-41-2009, 2009.
- 15 Bromwich, D. H., Nicolas, J. P., and Monaghan, A. J.: An assessment of precipitation changes over Antarctica and the Southern Ocean since 1989 in contemporary global reanalyses, *J. Climate*, 1406, 1–62, 2011.
- Chapman, L. W. and Walsh, J. E.: A synthesis of Antarctic temperatures, *J. Climate*, 2007, 20, 4096–4117, 2007.
- 20 Cheng, B., Zhang, Z., Vihma, T., Johansson, M., Bian, L., Li, Z., and Wu, H.: Model experiments on snow and ice thermodynamics in the Arctic Ocean with CHINARE 2003 data, *J. Geophys. Res.*, 113, 1–15, 2008.
- Comiso, J. C.: Variability and trends in Antarctic surface temperatures from in situ and satellite infrared measurements, *J. Climate*, 13, 1674–1696, 2000.
- 25 Cook, A. J. and Vaughan, D. G.: Overview of areal changes of the ice shelves on the Antarctic Peninsula over the past 50 years, *The Cryosphere*, 4, 77–98, doi:10.5194/tc-4-77-2010, 2010.
- Cook, A. J., Fox, A. J., Vaughan, D. G., and Ferrigno, J. G.: Retreating glacier fronts on the Antarctic Peninsula over the past half-century, *Science*, 308, 541–544, 2005.
- 30 Cooper, A. P. R.: Historical observations of Prince Gustav Ice Shelf, *Polar Record*, 33, 285–294, 1997.

Title Page

Abstract

Introduction

Conclusions

References

Tables

Figures

◀

▶

◀

▶

Back

Close

Full Screen / Esc

Printer-friendly Version

Interactive Discussion



## Results based on reanalyses in 1989–2010

I. Välisuo et al.

Title Page

Abstract

Introduction

Conclusions

References

Tables

Figures

◀

▶

◀

▶

Back

Close

Full Screen / Esc

Printer-friendly Version

Interactive Discussion



- Cullather, R. I. and Bosilowich, M. G.: The energy budget of the Polar atmosphere in MERRA, *J. Climate*, 25, 5–24, 2012.
- De Angelis H. and Skvarca P: Glacier surge after ice shelf collapse, *Science*, 299, 1560–1562, 2003.
- 5 Dee, D., Uppala, S. M., Simmons, A. J., Berrisford, P., Poli, P., Kobayashi, S., Andrae, U., Balmaseda, M. A., Balsamo, G., Bauer, P., Bechtold, P., Beljaars., A. C. M., van de Berg, L., Bidlot, J., Bormann, N., Delsol, C., Dragani, R., Fuentes., M., Geer, A. J., Haimberger, L., Healy, S. B., Hersbach, H., Hólm, E. V., Isaksen, L., Kållberg, P., Köhler, M., Matricardi, M., McNally, A. P., Monge-Sanz, B. M., Morcrette, J.-J., Park, B.-K., Peubey, C., de Rosnay, P.,  
10 Tavolato, C., Thépaut, J.-N., and Vitart, F.: The ERA-Interim reanalysis: configuration and performance of the data assimilation system, *Q. J. R. Meteorol. Soc.*, 137, 553–597, 2011.
- Glasser, N. F. and Scambos, T. A.: A structural glaciological analysis of the 2002 Larsen B ice shelf collapse, *J. Glaciol.*, 54, 3–16, 2008.
- Glasser, N. F., Kulesa, B., Luckman, A., Jansen, D., King, E. C., Sammond, P. R., Scambos, T. A., and Jezek, K. C.: Surface structure and stability of the Larsen C ice shelf, Antarctic Peninsula, *J. Glaciol.*, 55, 400–410, 2009.
- 15 Hodges, K. I., Lee, R. W., and Bengtsson, L.: A comparison of extra-tropical cyclones in recent re-analyses; ERA-INTERIM, NASA-MERRA, NCEP-CFSR and JRA25., *J. Climate*, 24, 4888–4906, 2011.
- 20 Jakobson, E., Vihma, T., Palo, T., Jakobson, L., Keernik, H., and Jaagus, J.: Validation of atmospheric reanalyses over the central Arctic Ocean, *Geophys. Res. Lett.*, 39, 1–6, 2012.
- Jansen, D., Kulesa, B., Sammonds, P. R., Luckman, A., King, J. C., and Glasser, N. F.: Present stability of the Larsen C ice shelf, Antarctic Peninsula, *J. Glaciol.*, 56, 593–600, 2010.
- Jones, P. D.: Recent variations in mean temperature and the diurnal temperature range in the Antarctic, *Geophys. Res. Lett.*, 22, 1345–1348, 1995.
- 25 King, J. C.: Recent climate variability in the vicinity of the Antarctic Peninsula, *Int. J. Climatol.*, 14, 357–369, 1994.
- King, J. C. and Turner, J.: *Antarctic Meteorology and Climatology*, Cambridge University Press, Cambridge, United Kingdom, 1997.
- 30 Kuipers Munneke, P., van den Broeke, M. R., King, J. C., Gray, T., and Reijmer, C. H.: Near-surface climate and surface energy budget of Larsen C ice shelf, Antarctic Peninsula, *The Cryosphere*, 6, 353–363, doi:10.5194/tc-6-353-2012, 2012.

**Results based on  
reanalyses in  
1989–2010**

I. Välisuo et al.

Title Page

Abstract

Introduction

Conclusions

References

Tables

Figures

◀

▶

◀

▶

Back

Close

Full Screen / Esc

Printer-friendly Version

Interactive Discussion



- Lucchita, K. B. and Rosanova, C. E.: Retreat of northern margins of George VI and Wilkins Ice Shelves, Antractic Peninsula, *Ann. Glaciol.*, 27, 41–46, 1998.
- Marshall, G. J., Orr, A., van Lipzig, N. P. M., and King, J. C.: The impact of a changing Southern Hemisphere annular mode on Antarctic Peninsula summer temperatures, *J. Climate*, 19, 5388–5404, 2006.
- 5 Mercer, J. H.: West Antarctic Ice Sheet and CO<sub>2</sub> greenhouse effect: a threat of disaster, *Nature*, 271, 321–325, 1978.
- Morris, E. M. and Vaughan, D. G.: Spatial and temporal variation of surface temperature on the Antarctic Peninsula and the limit of viability of ice shelves, *Antarc. Res. Ser.*, 79, 61–68, 2003.
- 10 Onogi, K., Tsutsui, J., Koide, H., Sakamoto, M., Kobayashi, S., Hatsushika, H., Matsumoto, T., Yamazaki, N., Kamahori, H., Takahashi, K., Kadokura, S., Wada, K., Kato, K., Oyama, R., Ose, T., Mannoji, N., and Taira, R.: The JRA-25 Reanalysis, *Journal of Meteorological Society of Japan*, 85, 369–432, 2007.
- 15 Orr, A., Cresswell, D., Marshall, G. J., Hunt, J. C. R., Sommeria, J., Wang, C. G., Light, M.: A “low-level” explanation for the recent large warming trend over the western Antarctic Peninsula involving blocked winds and changes in zonal circulation, *Geophys. Res. Lett.*, 31, L06204, doi:10.1029/2003GL019160, 2004.
- Rignot, E., Casassa, G., Gogineni, P., Krabill, W., Rivera, A., and Thomas, R.: Accelerated ice discharge from the Antarctic Peninsula following the collapse of Larsen B ice shelf, *Geophys. Res. Lett.*, 31, L18401, doi:10.1029/2004GL020697, 2004.
- 20 Rott, H., Skvarca, P., and Nagler, T.: Rapid collapse of northern Larsen Ice Shelf, *Antarctica, Science*, 271, 788–792, 1996.
- Rott, H., Rack, W., Nagler, T., and Skvarca, P.: Climatically induced retreat and collapse of northern Larsen Ice Shelf, *Antarctic Peninsula, Ann. Glaciol.*, 27, 86–92, 1998.
- 25 Rott, H., Rack, W., Skvarca, P., and De Angelis, H.: Northern Larsen Ice Shelf, Antarctica: further retreat and collapse, *Ann. Glaciol.*, 34, 277–282, 2002.
- Rott, H., Müller, F., Nagler, T., and Floricioiu, D.: The imbalance of glaciers after disintegration of Larsen-B ice shelf, *Antarctic Peninsula, The Cryosphere*, 5, 125–134, doi:10.5194/tc-5-125-2011, 2011.
- 30 Saha, S., Moorthi, S., Pan, H.-L., Wu, X., Wang, J., Nadiga, S., Tripp, P., Kistler, R., Woollen, J., Behringer, D., Liu, H., Stokes, D., Grumbine, R., Gayno, G., Wang, J., Hou, Y.-T., Chuang, H.-Y., Juang, H.-M. H., Sela, J., Iredell, M., Treadon, R., Kleist, D., Van Delst, P., Keyser, D.,

## Results based on reanalyses in 1989–2010

I. Välisuo et al.

Title Page

Abstract

Introduction

Conclusions

References

Tables

Figures

◀

▶

◀

▶

Back

Close

Full Screen / Esc

Printer-friendly Version

Interactive Discussion

Derber, J., Ek, M., Meng, J., Wei, H., Yang, R., Lord, S., van den Dool, H., Kumar, A., Wang, W., Long, C., Chelliah, M., Xue, Y., Huang, B., Schemm, J.-K., Ebisuzaki, W., Lin, R., Xie, P., Chen, M., Zhou, S., Higgins, W., Zou, C.-Z., Liu, Q., Chen, Y., Han, Y., Cucurull, L., Reynolds, R. W., Rutledge, G., and Goldberg, M.: The NCEP Climate Forecast System Reanalysis, *B. Am. Meteor. Soc.*, 91, 1015–1057, 2010.

Sansom, J.: Antarctic surface temperature time series, *J. Climate*, 2, 1168–1172, 1989.

Scambos, T. A., Hulbe, C., Fahnestock, M., and Bohlander, J.: The link between climate warming and break-up of ice shelves in the Antarctic Peninsula, *J. Glaciol.*, 46, 516–530, 2000.

Scambos, T. A., Hulbe, C., and Fahnestock, M.: Climate induced ice shelf disintegration in the Antarctic Peninsula, *Antarc. Res. Ser.*, 76, 335–347, 2003.

Shepherd, A., Wingham, D., Payne, T., and Skvarca, P.: Larsen Ice Shelf has progressively thinned, *Science*, 302, 856–859, 2003.

Singh, P. and Singh, V. P.: *Snow and Glacier Hydrology*, Kulwer Academic Publisher, Dordrech, the Netherlands, 2001.

Skvarca, P.: Fast recession of the northern Larsen Ice Shelf monitored by space images, *Ann. Glaciol.*, 17, 317–321, 1993.

Skvarca, P.: Changes and surface features of the Larsen Ice Shelves, Antarctica, derived from Landsat and Kosmos mosaics, *Ann. of Glaciol.*, 20, 6–12, 1994.

Skvarca, P., Rack, W., Rott, H., and Ibarzabal y Donangelo, T.: Evidence of recent climatic warming on the eastern Antarctic Peninsula, *Ann. Glaciol.*, 27, 628–632, 1998.

Skvarca, P., Rack, W., Rott, H., and Ibarzabal y Donangelo, T.: Climatic trend and the retreat and disintegration of ice shelves on the Antarctic Peninsula: an overview, *Polar Res.* 18, 151–157, 1999.

Stössel, A., Zhang, Z., and Vihma, T.: The effect of alternative real-time wind forcing on Southern Ocean sea ice simulations, *J. Geophys. Res.*, 116, C11021, doi:10.1029/2011JC007328, 2011.

Turner, J., Colwell, S. R., Marshall, G. J., Lachlan-Cope, T. A., Carleton, M., Jones, P. D., Lagun, V., Reid, P. A., and Iagovkina, S.: Antarctic climate change during the last 50 years, *Int. J. Climatol.*, 25, 279–294, 2005.

van den Broeke, M.: Strong surface melting preceded collapse of Antarctic Peninsula ice shelf, *Geophys. Res. Lett.*, 32, L12815, doi:10.1029/2005GL023247, 2005.

van Lipzig, N. P. M., Marshall, G. J., Orr, A., King, J. C.: The relationship between the Southern Hemisphere annular mode and antarctic peninsula summer temperatures: analysis of a high-resolution model climatology, *J. Climate*, 21, 1649–1668, 2008.

5 Vaughan, D. G. and Doake, C. S. M.: Recent atmospheric warming and retreat of ice shelves on the Antarctic Peninsula, *Nature*, 379, 328–331, 1996.

Vaughan, D. G., Marshall, G. J., Connolley, W. M., Parkinson, C., Mulvaney, R., Hodgson, D. A., King, J. C., Pudsey, C. J., and Turner, J.: Recent rapid regional climate warming on the Antarctic Peninsula, *Climatic Change*, 60, 243–274, 2003.

10 Vihma, T., Uotila, J., Cheng, B., and Launiainen, J.: Surface heat budget over Weddell Sea: buoy results and model comparisons, *J. Geophys. Res.*, 107, doi:10.1029/2000JC000372, 2002.

TCD

7, 1269–1311, 2013

Results based on  
reanalyses in  
1989–2010

I. Välisuo et al.

Title Page

Abstract

Introduction

Conclusions

References

Tables

Figures

◀

▶

◀

▶

Back

Close

Full Screen / Esc

Printer-friendly Version

Interactive Discussion



## Results based on reanalyses in 1989–2010

I. Välisuo et al.

**Table 1.** Validation of reanalyses against AWS observations on LCIS. The correlations are calculated for inter-annual variations of seasonal means.

		ERA-Interim			JRA-55			CFRSR		
		<i>R</i>	Bias	RMSE	<i>R</i>	Bias	RMSE	<i>R</i>	Bias	RMSE
Temperature	DJF	0.43	2.4	3.0	0.51	1.3	2.3	0.61	-0.7	1.9
	MAM	0.25	5.3	5.8	-0.04	4.7	2.3	0.09	3.2	4.7
	JJA	0.71	4.9	5.4	0.39	3.6	5.8	0.21	3.0	4.5
	SON	0.53	3.3	4.0	0.29	2.7	5.1	0.49	1.3	2.6
<i>U</i>	DJF	0.46	0.5	0.8	0.63	0.6	1.0	-0.10	0.6	0.9
	MAM	0.03	1.1	1.6	0.15	0.2	1.3	0.13	0.4	0.9
	JJA	0.37	1.4	1.6	0.39	0.6	1.3	0.11	0.4	1.3
	SON	-0.14	1.0	1.7	0.09	1.2	2.0	-0.07	0.6	0.9
<i>V</i>	DJF	0.37	-0.2	0.7	0.36	0.5	0.8	0.43	0.3	0.8
	MAM	0.56	-0.9	1.1	0.03	-0.4	1.2	0.37	-0.9	1.2
	JJA	0.33	-0.6	1.0	0.10	0.1	1.0	0.26	-0.5	1.0
	SON	0.07	-0.8	1.1	0.17	-0.3	0.9	0.25	-0.6	1.0

Title Page

Abstract

Introduction

Conclusions

References

Tables

Figures

◀

▶

◀

▶

Back

Close

Full Screen / Esc

Printer-friendly Version

Interactive Discussion



## Results based on reanalyses in 1989–2010

I. Välisuo et al.

**Table 2.** Seasonal mean values of the surface fluxes on Larsen C and Wilkins ice shelves.

	ERA-Interim (ERA-I)					JRA-55					Climate Forecast System Reanalysis (CFSR)				
	LW	SW	SH	LH	NF	LW	SW	SH	LH	NF	LW	SW	SH	LH	NF
LCIS															
DJF	-43	59	3	-9	10	-50	84	4	-11	26	-36	52	9	-19	7
MAM	-28	8	9	-2	-13	-39	12	8	-1	-10	-31	9	23	-4	-3
JJA	-31	1	15	-1	-15	-40	2	24		-14	-33	1	30	-4	-5
SON	-42	33	9	-6	-6	-51	46	14	-6	3	-40	34	18	-12	1
Ann.	-36	25	9	-4	-6	-45	36	15	-4	2	-35	24	20	-9	0
WIS															
DJF	-42	59	2	-10	8	-51	102	4	-13	41	-37	60	9	-14	28
MAM	-32	8	7	-4	-21	-39	12	22	-3	-9	-28	9	18	-8	-30
JJA	-29	1	8	-2	-21	-41	1	25		-15	-28	1	18	-7	37
SON	-37	27	4	-6	-12	-51	50	15	-9	5	-35	34	13	-13	0
Ann.	-35	24	5	-5	-12	-46	41	16	-6	5	-32	26	15	-11	-10

Title Page

Abstract Introduction

Conclusions References

Tables Figures

◀ ▶

◀ ▶

Back Close

Full Screen / Esc

Printer-friendly Version

Interactive Discussion



## Results based on reanalyses in 1989–2010

I. Välisuo et al.

**Table 3.** Statistically significant (95 %) seasonal and annual trends on LCIS during the period from 1989 to 2010 for Mars, April, May (MAM), June, July, August (JJA), September, October, November (SON), and December, January, February (DJF). Abbreviations are for net longwave radiation (LW), sensible heat flux (SH), latent heat flux (LH), net flux (NF), temperature 2 m above the surface ( $T$ ), eastward wind component ( $U$ ) and northward wind component ( $V$ ). The units in the table are for the fluxes  $\text{W m}^{-2} \text{yr}^{-1}$ ;  $^{\circ}\text{C yr}^{-1}$  and  $(\text{m s}^{-1} \text{yr}^{-1})$  for the wind.

		ERA-Interim					JRA-55				CFRSR			
LCIS		LW	SH	LH	NF	$T$	$V$	LH	NF	$T$	LW	LH	NF	$U$
DJF		-0.44						0.04	-0.37					0.03
MAM				-0.12	-0.55								0.13	
JJA													0.16	
SON								-0.07					0.10	
Ann.							0.05						0.10	
<hr/>														
LCIS		LW	SH	LH	NF	$T$	$V$	LH	NF	$T$	LW	LH	NF	$U$
DJF			-0.15	-0.10				0.22						0.03
MAM		-0.36		-0.16	-0.55			0.12	0.21	0.13				
JJA		-0.41	-0.27	-0.09	-0.78	0.23							-0.21	
SON			-0.27	-0.22	-0.74									
Ann.		-0.22	-0.18	-0.14				0.09			0.17	-0.10		0.03

[Title Page](#)
[Abstract](#)
[Introduction](#)
[Conclusions](#)
[References](#)
[Tables](#)
[Figures](#)
[◀](#)
[▶](#)
[◀](#)
[▶](#)
[Back](#)
[Close](#)
[Full Screen / Esc](#)
[Printer-friendly Version](#)
[Interactive Discussion](#)


## Results based on reanalyses in 1989–2010

I. Välisuo et al.

**Table 4.** Mean cloud fraction (TCC), downward thermal (LW\_down) and solar radiation (SW\_down) and net radiation (R\_net) on LCIS surface in selected seasons.

	Winter 1991	Winter 1996	Summer 92–93	Summer 99–00
TCC (%)	68	78	75	67
LW_down ( $Wm^{-2}$ )	196	213	271	257
SW_down ( $Wm^{-2}$ )	5	4	242	273
R_net ( $Wm^{-2}$ )	–42	–27	41	13

[Title Page](#)
[Abstract](#)
[Introduction](#)
[Conclusions](#)
[References](#)
[Tables](#)
[Figures](#)
[Back](#)
[Close](#)
[Full Screen / Esc](#)
[Printer-friendly Version](#)
[Interactive Discussion](#)

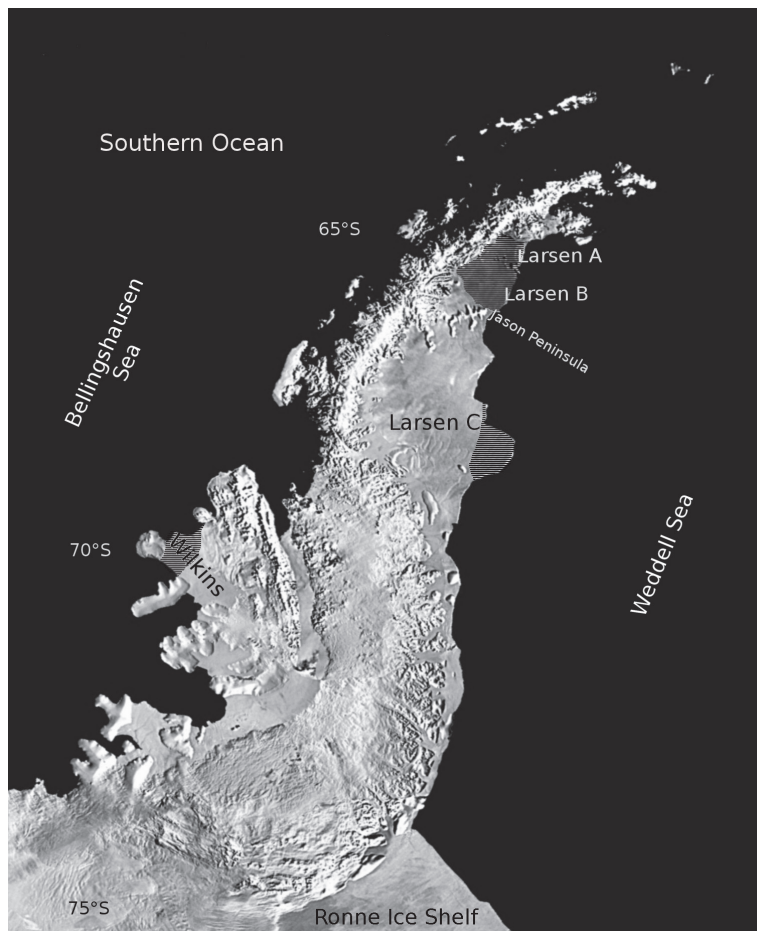

## Results based on reanalyses in 1989–2010

I. Välisuo et al.

**Table 5.** Multiple regression equations and explanation levels for surface net flux (NF) explained by weather variables: mean sea level air pressure ( $p$ , in hPa); 10-m wind speed ( $UV$ , in  $\text{ms}^{-1}$ ), eastward wind component ( $U$ ), northward wind component ( $V$ ), and the cloud fraction ( $N$ , 0–1).

Region	Period	Multiple regression equation	$r^2$	RMSE
Larsen C	DJF	$NF = -5.5V + 8.4UV + 0.6p - 626$	0.79	3.2
Larsen C	MAM	$NF = 3.4V + 0.6p - 3.6UV - 104$	0.58	5.0
Larsen C	JJA	$NF = 9.2U + 158.5N + 1.0p - 5.6UV - 1126$	0.80	4.5
Wilkins	MAM	$NF = 3.0U - 18$	0.26	4.5
Wilkins	JJA	$NF = 79.9N - 88$	0.27	7.0

[Title Page](#)
[Abstract](#)
[Introduction](#)
[Conclusions](#)
[References](#)
[Tables](#)
[Figures](#)
[◀](#)
[▶](#)
[◀](#)
[▶](#)
[Back](#)
[Close](#)
[Full Screen / Esc](#)
[Printer-friendly Version](#)
[Interactive Discussion](#)

**Fig. 1.** Antarctic Peninsula. Modified from NASA's Blue Marble data set (MODIS AVHRR). The disintegrated parts of Larsen and Wilkins ice shelves are marked with thin stripes.

Results based on reanalyses in 1989–2010

I. Välisuo et al.

Title Page

Abstract Introduction

Conclusions References

Tables Figures

◀ ▶

◀ ▶

Back Close

Full Screen / Esc

Printer-friendly Version

Interactive Discussion



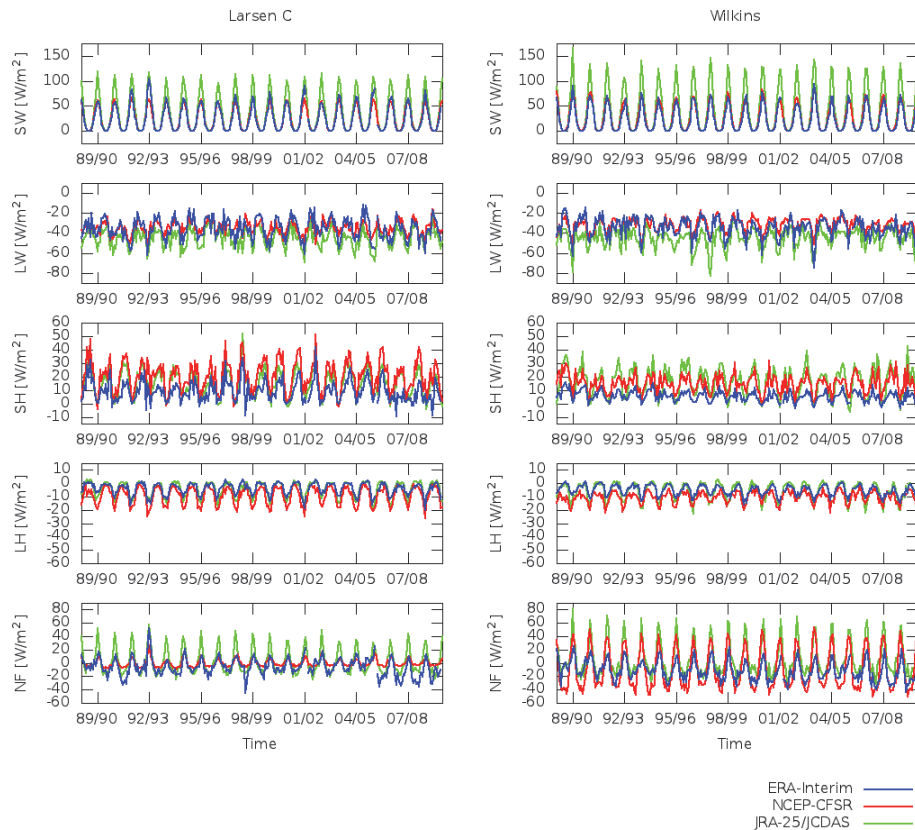


**Fig. 2.** Time series of monthly mean surface energy fluxes on Larsen C and Wilkins ice shelves based on ERAI, CFSR, and JRA reanalyses.

Title Page

Abstract

Introduction

Conclusions

References

Tables

Figures

◀

▶

◀

▶

Back

Close

Full Screen / Esc

Printer-friendly Version

Interactive Discussion



## Results based on reanalyses in 1989–2010

I. Välisuo et al.

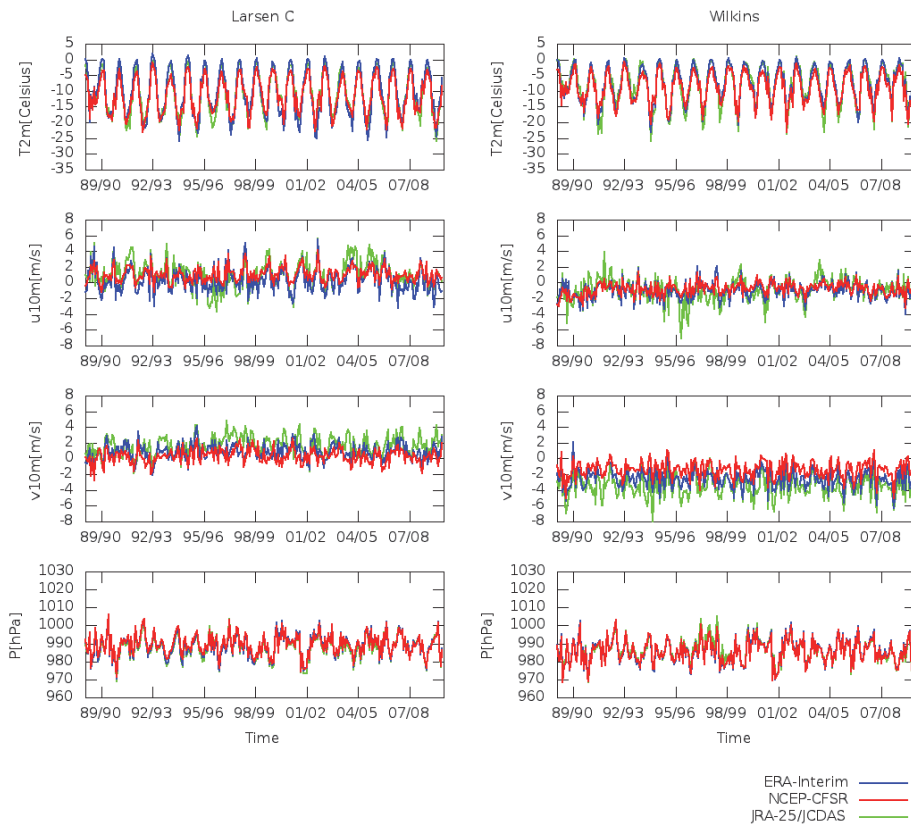


**Fig. 3.** Time series of 2 m air temperature, 10 m wind speed and mean sea level pressure on Larsen C and Wilkins Ice Shelves on the basis of ERAI, CFSR, and JRA reanalyses.

[Title Page](#)
[Abstract](#)
[Introduction](#)
[Conclusions](#)
[References](#)
[Tables](#)
[Figures](#)
[◀](#)
[▶](#)
[◀](#)
[▶](#)
[Back](#)
[Close](#)
[Full Screen / Esc](#)
[Printer-friendly Version](#)
[Interactive Discussion](#)


Results based on  
reanalyses in  
1989–2010

I. Välisuo et al.

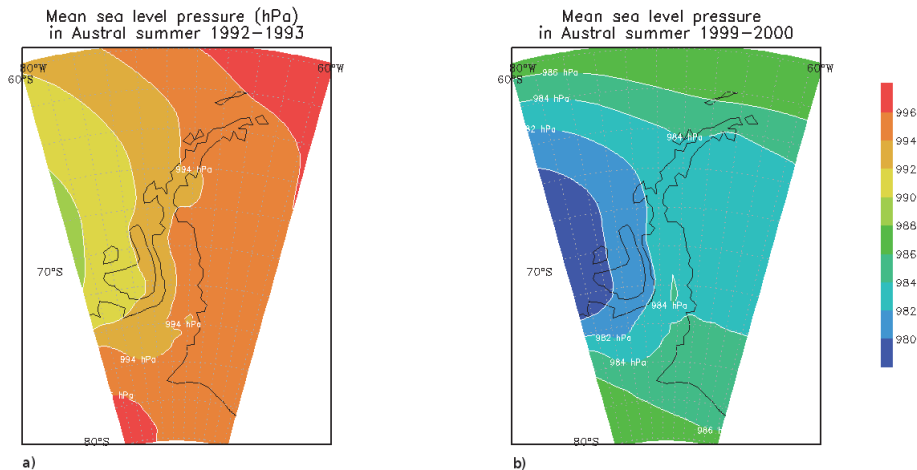


**Fig. 4.** Mean sea level pressure (hPa) in austral summers 1992–1993 (a) and 1999–2000 (b) on the basis of ERA-Interim reanalysis.

Title Page

Abstract

Introduction

Conclusions

References

Tables

Figures

◀

▶

◀

▶

Back

Close

Full Screen / Esc

Printer-friendly Version

Interactive Discussion

## Results based on reanalyses in 1989–2010

I. Välisuo et al.

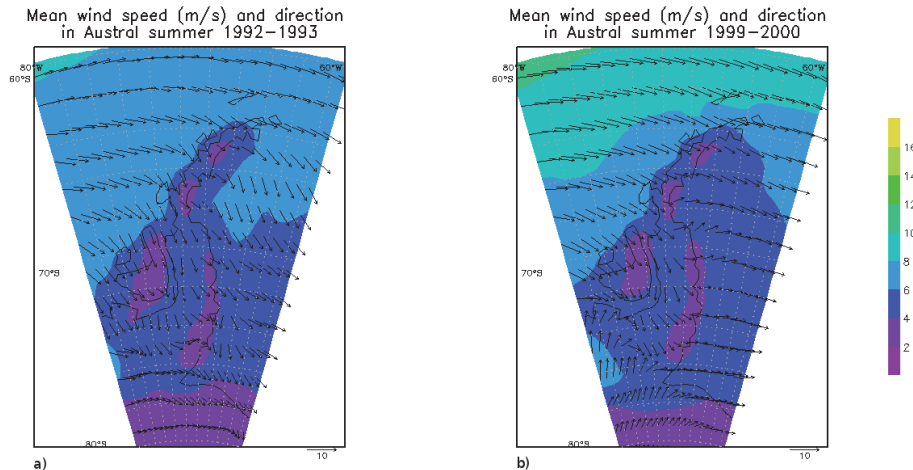


**Fig. 5.** Mean wind speed ( $\text{ms}^{-1}$ ) and direction in austral summers 1992–1993 **(a)** and 1999–2000 **(b)** on the basis of ERA-Interim reanalysis.

[Title Page](#)[Abstract](#)[Introduction](#)[Conclusions](#)[References](#)[Tables](#)[Figures](#)[◀](#)[▶](#)[◀](#)[▶](#)[Back](#)[Close](#)[Full Screen / Esc](#)[Printer-friendly Version](#)[Interactive Discussion](#)

**Results based on  
reanalyses in  
1989–2010**

I. Välisuo et al.

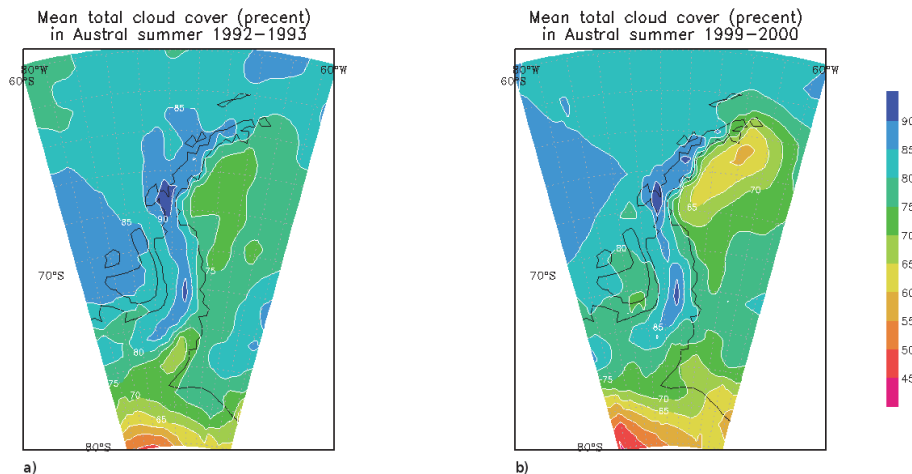


**Fig. 6.** Mean cloud fraction in austral summers 1992–1993 **(a)** and 1999–2000 **(b)** on the basis of ERA-Interim reanalysis.

Title Page

Abstract

Introduction

Conclusions

References

Tables

Figures

◀

▶

◀

▶

Back

Close

Full Screen / Esc

Printer-friendly Version

Interactive Discussion



Results based on  
reanalyses in  
1989–2010

I. Välisuo et al.

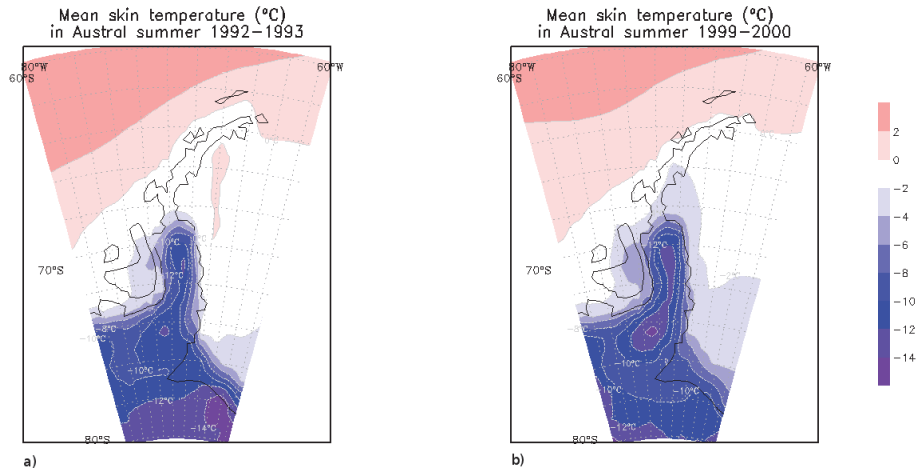


**Fig. 7.** Mean skin temperature in austral summers 1992–1993 (a) and 1999–2000 (b) on the basis of ERA-Interim reanalysis.

Title Page

Abstract

Introduction

Conclusions

References

Tables

Figures

◀

▶

◀

▶

Back

Close

Full Screen / Esc

Printer-friendly Version

Interactive Discussion



Title Page

Abstract

Introduction

Conclusions

References

Tables

Figures



Back

Close

Full Screen / Esc

Printer-friendly Version

Interactive Discussion

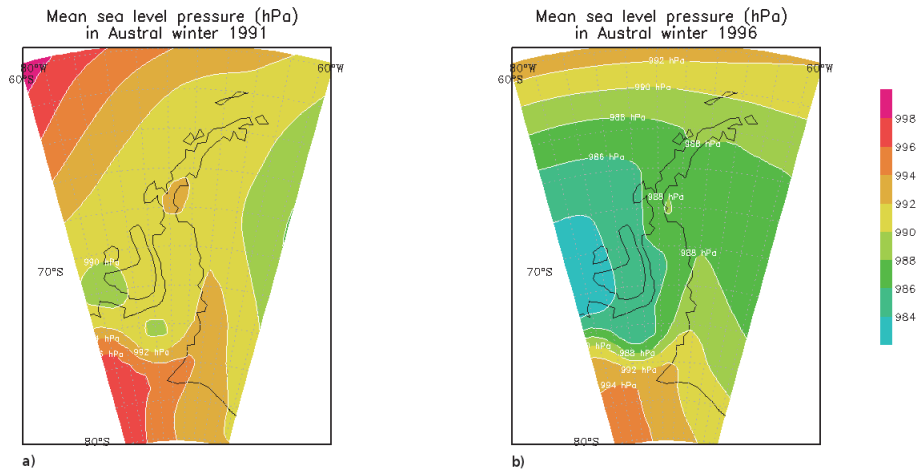


**Fig. 8.** Mean sea level pressure in austral winters 1991 (a) and 1996 (b) on the basis of ERA-Interim reanalysis.

## Results based on reanalyses in 1989–2010

I. Välisuo et al.

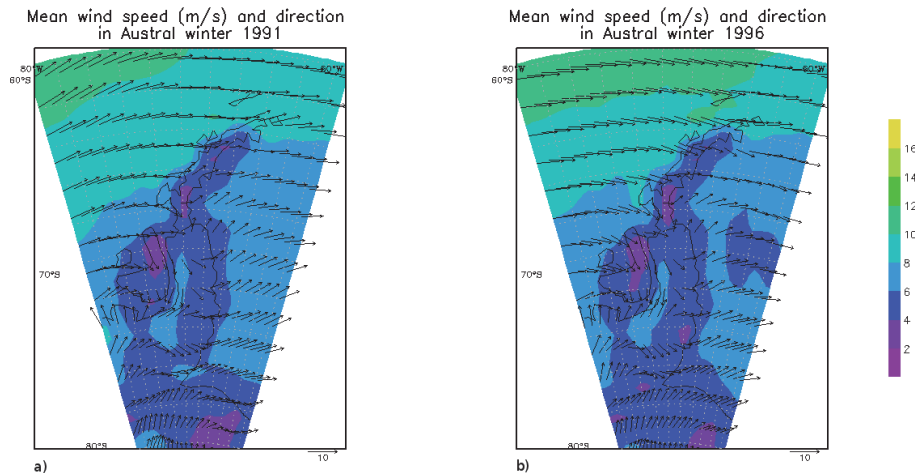


**Fig. 9.** Mean wind speed and direction in winters 1991 **(a)** and 1996 **(b)** on the basis of ERA-Interim reanalysis.

Title Page

Abstract

Introduction

Conclusions

References

Tables

Figures

◀

▶

◀

▶

Back

Close

Full Screen / Esc

Printer-friendly Version

Interactive Discussion



Results based on  
reanalyses in  
1989–2010

I. Välisuo et al.

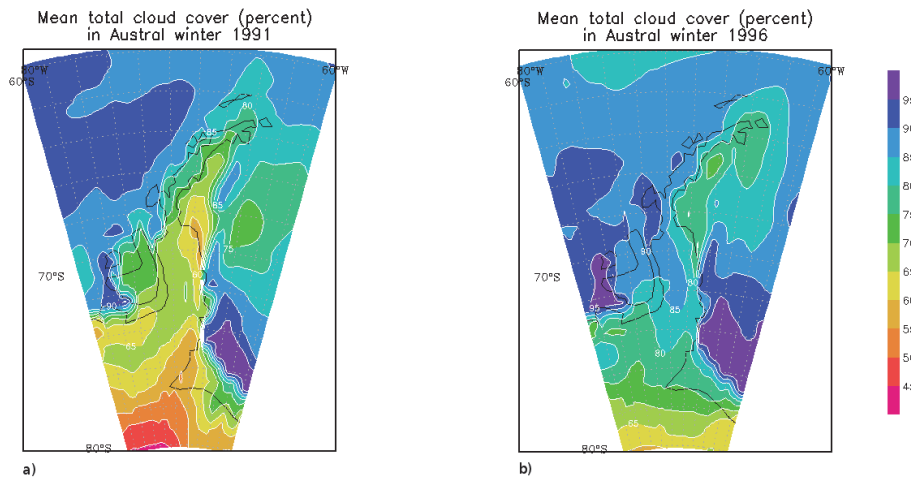


**Fig. 10.** Mean cloud fraction in austral winters 1991 (a) and 1996 (b) on the basis of ERA-Interim reanalysis.

Title Page

Abstract

Introduction

Conclusions

References

Tables

Figures

◀

▶

◀

▶

Back

Close

Full Screen / Esc

Printer-friendly Version

Interactive Discussion



Results based on  
reanalyses in  
1989–2010

I. Välisuo et al.

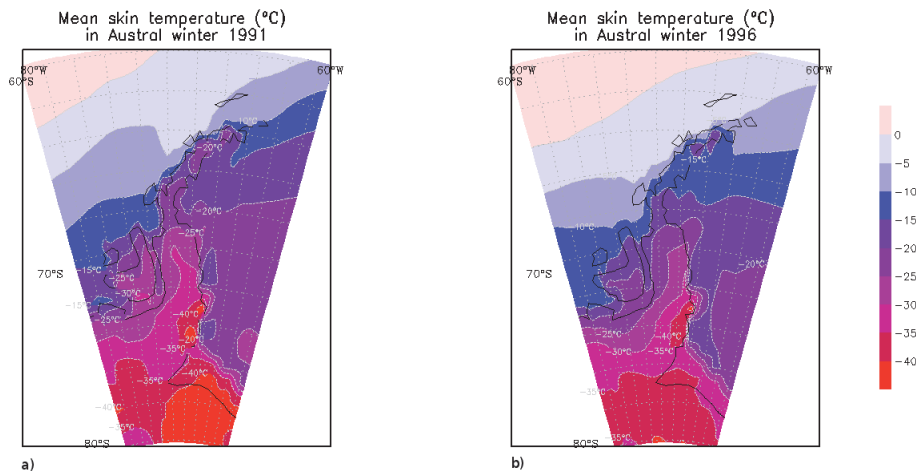


**Fig. 11.** Mean skin temperature in winters 1991 (a) and 1996 (b) on the basis of ERA-Interim reanalysis.

[Title Page](#)[Abstract](#)[Introduction](#)[Conclusions](#)[References](#)[Tables](#)[Figures](#)[◀](#)[▶](#)[◀](#)[▶](#)[Back](#)[Close](#)[Full Screen / Esc](#)[Printer-friendly Version](#)[Interactive Discussion](#)

## Results based on reanalyses in 1989–2010

I. Välisuo et al.

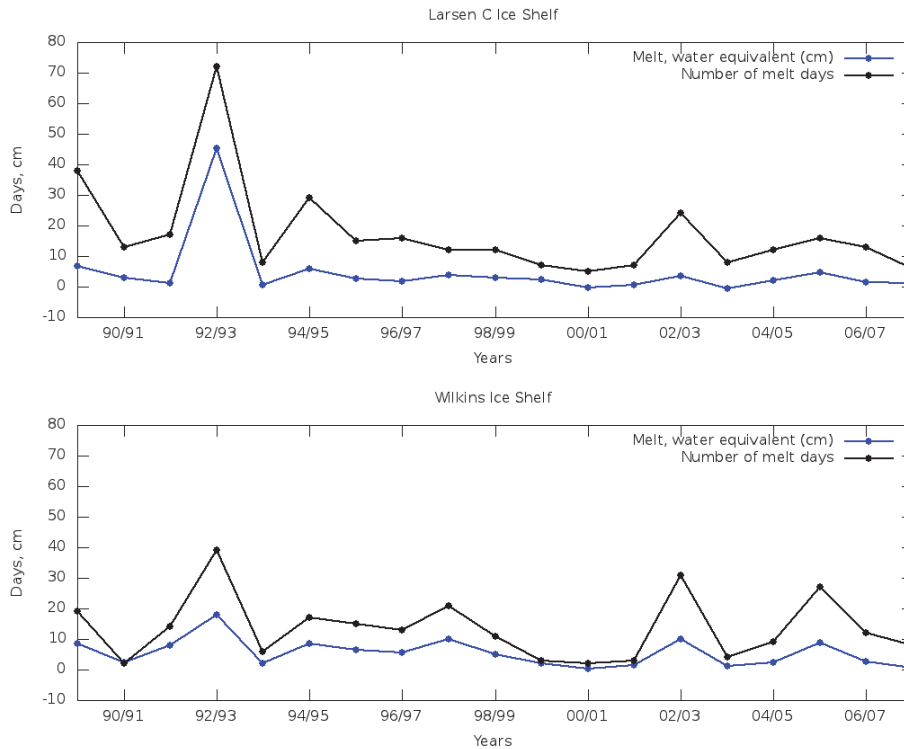


**Fig. 12.** Mean summertime melting and number of melt days on Larsen C and Wilkins ice shelves calculated on the basis of ERA-Interim reanalysis.

[Title Page](#)
[Abstract](#)
[Introduction](#)
[Conclusions](#)
[References](#)
[Tables](#)
[Figures](#)
[◀](#)
[▶](#)
[◀](#)
[▶](#)
[Back](#)
[Close](#)
[Full Screen / Esc](#)
[Printer-friendly Version](#)
[Interactive Discussion](#)
